

Washington University School of Medicine

Digital Commons@Becker

Open Access Publications

2020

Identification of the growth factor-binding sequence in the extracellular matrix protein MAGP-1

Thomas J. Broekelmann

Nicholas K. Bodmer

Robert P. Mecham

Follow this and additional works at: https://digitalcommons.wustl.edu/open_access_pubs

Identification of the growth factor binding sequence in the extracellular matrix protein MAGP-1

Thomas J. Broekelmann, Nicholas K. Bodmer, and Robert P. Mecham*

From the Department of Cell Biology and Physiology, Washington University School of Medicine, St. Louis, MO 63110

Running Title: *TGF β binding sequence in MAGP-1*

* To whom correspondence should be address: Robert Mecham, Department of Cell Biology and Physiology, Campus Box 8228, 660 South Euclid Ave, St. Louis, MO 63110; bmecham@wustl.edu;

Keywords: microfibril, microfibril-associated glycoprotein (MAGP), MFAP2, TGF β , bone morphogenetic protein (BMP), fibrillin, extracellular cellular matrix (ECM), growth factor signaling, protein-protein interaction

ABSTRACT

Microfibril-associated glycoprotein-1 (MAGP-1) is a component of vertebrate extracellular matrix (ECM) microfibrils that, together with the fibrillins, contributes to microfibril function. Many of the phenotypes associated with *MAGP-1* gene inactivation are consistent with dysregulation of the transforming growth factor β (TGF β)/bone morphogenetic protein (BMP) signaling system. We have previously shown that full-length MAGP-1 binds active TGF β -1 and some BMPs. The work presented here further defines the growth factor-binding domain of MAGP-1. Using recombinant domains and synthetic peptides, along with surface plasmon resonance analysis to measure the kinetics of the MAGP-1–TGF β -1 interaction, we localized the TGF β - and BMP-binding site in MAGP-1 to a 19-amino-acid-long, highly acidic sequence near the N terminus. This domain was specific for binding active, but not latent, TGF β 1. Growth factor activity experiments revealed that TGF β -1 retains signaling activity when complexed with MAGP-1. Furthermore, when bound to fibrillin, MAGP-1 retained the ability to interact with TGF β -1, and active TGF β -1 did not bind fibrillin in the absence of MAGP-1. The absence of MAGP was sufficient to raise the amount of total TGF β stored in the ECM of cultured cells, suggesting that the MAGPs compete with the TGF β large latent complex for binding to microfibrils. Together, these results indicate that MAGP-1 plays an active role in TGF β signaling in the ECM.

INTRODUCTION

The extracellular matrix (ECM) is a composite biomaterial that contains informational signals that influence cell phenotypes. The changing composition of the ECM during development and tissue repair provides necessary feedback signals used by cells to build functional tissues. Information from the ECM is transmitted to cells through direct interaction with specific receptors (e.g., integrins), through mechanical signals that reflect the material properties of the ECM and cellular microenvironment, and through regulation of growth factor accessibility and signaling. Many ECM proteins bind growth factors and regulate their activity by providing a pericellular substrate for presenting growth factors to specific receptors on cells or by sequestering active and latent forms away from the cell for later utilization (1). Growth factors bind to discrete domains and motifs in ECM proteins, and there is remarkable specificity to these binding interactions. As the ECM changes during development, so does the repertoire of ECM-associated growth factors that influence cell phenotypes.

The microfibril is an extracellular matrix structure made up of fibrillin as the core unit. Fibrillin appeared early in evolution and, over time, developed both structural and signaling functions (2). Fibrillin monomers assemble into

fibers of 12-15 nm diameter that provide strength to tissues by forming fiber bundles. An example includes the ciliary zonule in the eye, where microfibrils form the suspensory ligaments that support the lens (3,4). Microfibrils are also an important structural component of primitive vertebrate and invertebrate arteries where they provide a degree of elastic recoil (5-7).

Another key function of microfibrils is modulation of growth factor signaling through fibrillin interactions with the latent TGF β binding proteins (LTBPs). LTBPs covalently bind the small latent complex of TGF β to form the large latent TGF β complex (TGF β -LLC), which binds to fibrillin (8,9). By sequestering latent TGF β in the matrix, microfibrils indirectly regulate TGF β signaling by providing a store of inactive growth factor that can be utilized through activation by proteolysis or by mechanical strain (10).

With the arrival of vertebrates in evolution, new proteins appeared that interact with fibrillin and modify microfibrillar function. These include elastin and microfibril-associated glycoprotein-1 and -2 (MAGP-1 and MAGP-2). Elastic fiber formation requires microfibrils (11) and, because MAGP-1 can bind both tropoelastin (12,13) and fibrillin (14), the MAGPs were initially thought to promote the tropoelastin-microfibril interaction necessary for elastin assembly. However, inactivation of the genes for MAGP-1 and MAGP-2 in mice did not affect elastic fiber formation. Instead, mice lacking these proteins had abnormalities in bone, fat, hematopoiesis, and wound healing that were associated with abnormal TGF β signaling (15-17). We have previously documented a direct binding interaction between TGF β family growth factors and the MAGPs (18), but the sequence within MAGP that mediates this interaction was unknown. In this report, we localize the growth factor-binding domain in MAGP-1 to a sequence near the protein's amino terminus and address the functional consequences of the TGF β -MAGP interaction.

RESULTS

Characterization of recombinant purified full-length MAGP-1 and MAGP-1 fragments.

Full-length mouse MAGP-1 (exons 3-9) was expressed in *E-coli* along with a series of N-

terminal truncation mutants containing a N-terminal 6-His-tag. The truncations were based on the exon structure of the gene encoding the mature molecule shown in **Fig 1A** (the protein sequence for mouse MAGP-1 can be found in supporting information **Fig S1**). The gene for MAGP-1 contains nine exons, but only seven encode the secreted full-length protein. Exon 1 is untranslated, and exon 2 encodes the majority of the signal peptide, which is absent from the mature molecule. After confirming the correct sequence for each construct by DNA sequence analysis, the constructs were expressed, and the proteins purified. The results of the purification are shown in **Fig 1B**. The full-length protein has a predicted mass of 20.6 kDa, but by SDS-PAGE analysis migrates ~36 kDa. Similarly, the bacterially expressed domain 3-4 construct has a predicted mass of ~7.5 kDa but runs at approximately 16 kDa. Purified domain 4-9 runs slightly higher than expected (19 kDa compared to the predicted 17.5 kDa), and the domain 5-9 protein runs true to the predicted mass of ~16 kDa. Because the MAGP-1 protein and fragments are expressed in bacteria, the irregular migration is not due to post-translational modifications. Anomalous migration of full-length MAGP-1 on SDS-PAGE has been described (19). Our results suggest that the sequence within domains 3-4 is responsible for this irregular behavior.

TGF β binding to MAGP-1 fragments

Our goal in this study was to localize the region of MAGP-1 that interacts with TGF β growth factors. To this end, we performed a set of surface plasmon resonance (SPR) experiments where purified TGF β -1 was injected over immobilized full-length MAGP-1 or over the purified truncation fragments coupled to CM-5 sensor chips. **Fig 2A** shows binding isotherms for soluble TGF β -1 interacting with immobilized full-length MAGP-1 in the SPR-based assay. The affinity constant calculated using 1:1 Langmuir binding was 15nM. When tested for binding to the MAGP-1 fragments, TGF β -1 bound the domain 3-4 coupled sensor chip with a slightly higher affinity than the full-length protein, as seen in **Fig 2B**. The affinity constant calculated using 1:1 Langmuir binding was 3nM. Binding of TGF β -1 to domain 4-9 showed substantially

lower affinity (190nM), and there was no TGF β -1 binding to a chip coated with domain 5-9 (**Fig 2C and 2D**, respectively). These results suggest that the primary binding site for TGF β -1 is located in domain 4 of MAGP-1 with an affinity contribution from domain 3.

TGF β binds to a 19-residue peptide sequence spanning domains 3 and 4

Fine mapping of the MAGP-1 binding sequence for TGF β -1 was done using overlapping synthetic peptides that spanned the sequence encoded by exons 3 and 4. Each peptide was purified by high-pressure liquid chromatography, and the sequence confirmed by mass spectrometry (data not shown). Surprisingly, TGF β -1 failed to bind to a CM-5 sensor chip coated with a synthetic peptide made from the sequence of domain 3-4. The sequence was the same as the bacterially expressed domain 3-4 peptide except for an N-terminal 6-His-tag on the bacterially expressed protein. The 6-His-tag itself was not an active binding sequence since the expressed peptide 5-9 did not bind TGF β -1 even though it also had a 6-His-tag at the amino-terminus

Although unable to bind TGF β -1 when bound to a solid substrate, domain 3-4 synthetic peptide (p1-35) did inhibit binding of TGF β -1 to a full-length MAGP-1-coated sensor chip, thereby establishing its activity (supporting information **Fig S2A**). Therefore, for subsequent mapping studies, we used equilibrium titration experiments to assess the inhibitory activity of a series of peptides summarized in **Fig 3A**. The peptide based on the first 18 residues of domain 3 (p1-18) showed no inhibitory activity. A peptide derived from residues 22-36 (p22-36), and a domain 4 peptide (p26-35) both failed to inhibit TGF β -1 binding to full-length MAGP-1 (the inhibitory curve for peptide p22-36 is shown in supporting information **Fig S2B** as representative of no binding inhibition). A peptide with residues 12-37 (not shown) and a smaller peptide spanning residues 17-35 (p17-35), were both inhibitory.

A detailed investigation into the dose-response of the smallest peptide with inhibitory activity (p17-35) is shown in **Fig 3B**. There is a dose-dependent decrease in TGF β -1 binding to full-length MAGP-1, with half-maximal inhibition at approximately 30 μ M p17-35 (**Fig**

3C). These results are consistent with data from studies with recombinant MAGP-1 fragments and show that the TGF β -1 binding activity of MAGP-1 is defined by a 19 amino acid sequence in domains 3 and 4. A control peptide with conformational restraints containing four proline residues (p17-35pro) failed to inhibit TGF β -1 binding to full-length MAGP-1 (**Fig 3D**).

Secondary structure predictions for the MAGP-1 p17-35 peptide indicated that the sequence does not have extensive secondary structure elements, with most residues predicted to be a random coil (data not shown). IUPred results predicted a high degree of disorder from the primary sequence. PEP-FOLD models tended to be elongated or compact coils with little secondary structure. This region of the MAGP-1 protein is likely intrinsically disordered and cannot adopt an ordered state without binding to a binding partner such as a member of the TGF β superfamily.

MAGP-1 binds active, but not latent, TGF β -1

TGF β is produced as a disulfide-linked homodimer that is inactive due to the presence of the N-terminal latency-associated peptide. This small latent TGF β complex (SLC) is usually associated with LTBP1 to produce the large latent TGF β complex (LLC), which is covalently bound to fibrillin-containing microfibrils in the ECM (9). To determine if MAGP-1 interacts with latent TGF β -1, we injected the small latent complex form of TGF β -1 over a sensor chip coated with full-length MAGP-1. As shown in **Fig 4**, latent TGF β -1 at 15nM failed to bind to the full-length protein. However, after acid activation for 15 minutes, the same latent TGF β -1 preparation showed a robust interaction with MAGP-1.

Neither MAGP-1 nor p17-35 inhibits TGF β -1 signaling.

To investigate whether TGF β -1 can still interact with its cellular receptor when complexed with MAGP-1, we pre-mixed MAGP-1 or MAGP-1 fragments with active TGF β -1 and then added the complex to the reporter cell line MFB-F11. MFB-F11 cells are embryonic fibroblasts from *Tgfb1*^{-/-} embryos stably transfected with a reporter plasmid consisting of TGF β responsive Smad-binding elements coupled to a secreted alkaline

phosphatase reporter gene (20). The secreted alkaline phosphatase can be detected with a chemiluminescent substrate and provides a sensitive assay for TGF β activity. We found that full-length MAGP-1 does not influence TGF β -1-stimulated alkaline phosphatase release from the MFB-F11 reporter cells when tested over a wide range of MAGP-1 concentrations (**Fig 5A**). Similarly, MAGP-1 peptide p17-35 that blocks binding of TGF β -1 to full-length MAGP-1, presumably by binding to the MAGP-1 binding site on the growth factor, does not affect the signaling potential of TGF β -1 (**Fig 5B**).

The effects of MAGP-1 on TGF β activity were also investigated by assessing changes in the SMAD signaling pathway in RFL-6 cells. In agreement with the MFB-F11 reporter cell assay, pre-incubating TGF β -1 with soluble MAGP-1 did not inhibit RFL-6 TGF β -1-stimulated Smad-2 phosphorylation (**Fig 5C**). **Fig 5D** shows that Smad-2 phosphorylation is TGF β dose dependent in RFL-6 cells with minimal pSmad2 detected in the absence of TGF β .

Predicted MAGP-1 binding site on TGF β

Molecular docking experiments consistently placed the MAGP-1 peptide p17-35 in contact with the finger region of TGF β -1 (**Fig 6**). The peptide prefers to dock near a cluster of positive residues in this region (R94, K95, and K97) that are solvent-exposed and, hence, in a position to attract and bind the negatively charged MAGP-1 peptide. The MAGP-1 peptide remains a highly flexible coil even when bound, suggesting that binding occurs through a promiscuous charge-charge interaction between the highly positive region of TGF β -1 and the negative residues of MAGP-1. The critical positively charged residues are inaccessible in the inactive TGF β -LAP complex, due to the presence of the latency lasso in the straight-jacket region of the large latency-associated complex (21). Masking of the MAGP-1 binding site by the latency peptide explains why MAGP-1 binds active TGF β but not the small latent complex.

MAGP forms a ternary complex with fibrillin-2 and TGF β -1.

Fibrillin interacts with LTBP1 to covalently anchor the TGF β large latent complex into the ECM (9,22). Whether active TGF β -1 can bind to

fibrillin is unclear. To explore a possible binding interaction between the two proteins, we injected 50nM of active TGF β -1 over full-length fibrillin-2 immobilized on an SPR chip. Fibrillin-2 was purified from a baculoviral expression system and showed a single band by SDS-PAGE (supporting information **Fig S3**). **Fig 7A** shows that no significant interaction was detected between TGF β -1 and fibrillin-2. Soluble MAGP-1, however, bound tightly to fibrillin-2 with an apparent affinity constant of 100pM (**Fig 7B**). The binding curve fits 1:1 Langmuir binding with a noticeable slow dissociation rate of $-2.64 \times 10^4 \text{ s}^{-1}$ and a half-life of 2600 seconds. We took advantage of this slow release rate to follow MAGP-1 injection onto the fibrillin-2 chip with 50nM of TGF β -1 and found robust binding of the growth factor to the fibrillin-2-MAGP-1 complex (**Fig 7C**). That MAGP-1 mediated the interaction was established by inhibiting TGF β binding with the active MAGP-1 peptide p17-35 (**Fig 7C**). The binding of TGF β -1 to the MAGP-1-fibrillin-2 complex showed similar binding kinetics to TGF β -1 binding directly to a MAGP-1-coated chip (compare the top curve in **Fig 3B** to **Fig 7C**).

BMP-2 binds to the same MAGP-1 sequence as TGF β .

Our previous studies found that MAGP-1 bound to BMP-7 with an affinity approximately equal to TGF β (18). To determine whether other BMP-family members interact with MAGP-1, we performed SPR experiments with BMP-2. **Fig 8A** shows BMP-2 binding to MAGP-1 with an affinity of 25nM. The binding was inhibited by the active MAGP-1 peptide p17-35, suggesting that TGF β s and BMPs recognize the same sequence on the MAGP-1 protein. The control peptide p17-35pro (**Fig 8B**) and the N-terminal peptide p1-18 (not shown) both failed to inhibit BMP-2 binding to full-length MAGP-1. We were unable to determine if BMP-2 could form a ternary complex with fibrillin-2 and MAGP-1 because BMP-2 bound directly to fibrillin-2 with an affinity of 8nM (supporting information **Fig S4**).

Matrix devoid of MAGPs has higher TGF β incorporation

The majority of TGF β in the ECM is in the form

of the large latent complex bound to fibrillin. MAGP-1 and the large latent complex bind to the same region of fibrillin (23), suggesting a possible competition between the two proteins for binding to microfibrils. To determine if the absence of MAGP allows for more latent complex to accrue in the ECM, we compared total and active TGF β levels in cultures of fibroblasts from WT and MAGP knockout cells. Because MAGP-2 can also bind TGF β (16) and might compensate in the absence of MAGP-1, we evaluated TGF β levels in MAGP-1 and MAGP-2 knockout MEFs as well as MEFS from MAGP-1;MAGP-2 double knockout mice. After 14 days of culture, there was 2-3 times more total (latent plus active) TGF β activity in acid-activated cell-ECM extracts of all MAGP knockout cells compared to WT (**Fig 9 black bars**). TGF β activity detected without acid activation (indicative of active TGF β) was also increased in the single knockout cell lines but was significantly lower in the double knockout MEFS (**Fig 9 gray bars**). Quantitative PCR confirmed that TGF β expression was similar for WT and MAGP knockout cells. Cell number was also equivalent for all cell types (supporting information **Fig. S5**).

DISCUSSION

The bioavailability of active TGF β is tightly regulated at multiple levels, both inside and outside the cell. It is a crucial regulator of ECM production (24) yet, in turn, is influenced by the ECM itself in ways that provide spatiotemporal control of growth factor activity (1,25,26). In the ECM, TGF β family growth factors bind avidly to sulfated sugars on proteoglycans as well as to ECM proteins (1,26). Fibrillin-containing microfibrils are particularly important in modulating TGF β signaling and the mechanisms whereby microfibril-associated proteins regulate growth factor availability and activity are complex. We and others have shown that the fibrillin binding partners MAGP-1 and MAGP-2 work together with fibrillin to modulate TGF β availability in the ECM (16,27-29). Mutations in MAGP genes lead to phenotypes in mice and humans that are associated with abnormal growth factor signaling (15,16,18,30-33).

The MAGPs are functionally defined by the amino acid composition of their front and back halves. The back half of MAGP-1 contains 13 cysteine residues, the first seven of which define the matrix binding domain that mediates interactions with fibrillin (34,35). The matrix binding region is the only conserved structural motif shared with MAGP-2 and is conserved in all species of MAGP-1 and MAGP-2. The cysteine-free N-terminal half of MAGP-1 is acidic, enriched in proline, and contains tyrosine residues that undergo sulfation and threonine residues that are sites for O-glycosylation. Sequences in this region also mediate noncovalent interactions with tropoelastin (12,13), the α 3 chain of collagen VI (13), decorin (36), and biglycan (37). While secondary structure prediction algorithms suggest a random configuration for the amino terminal sequences, the absence of cysteine residues, the high negative charge density, and the binding of numerous proteins to this area of the molecule suggests a structure that is accessible and adaptable.

In this report, we used an overlapping peptide mapping strategy to localize the growth factor-binding domain to 19 amino acids in the N-terminal region of MAGP-1. The TGF β binding site is contained in domain 4 but requires a part of domain 3 for full affinity (**Fig. 2**). The binding sequence is highly acidic due to four aspartic acid residues, one glutamic acid, and three tyrosine residues that are sites for sulfation (with the sulfate group adding more negative charge). The acidic residues form a structural repeat, with each separated by two nonpolar amino acids. The functional significance of this repeating structure is not known. The high charge density at this site resembles characteristics of heparin, which binds TGF β with high affinity through negatively charged sulfated sugars that interact with lysine residues on TGF β (38). In fact, the predicted MAGP-1 binding site on TGF β is the same as that postulated for heparin (38,39). While the charged residues in MAGP-1 are important for growth factor binding, there are conformational and flexibility requirements as well, since the biologically active p17-35 peptide no longer interacts with TGF β when prolines are inserted to introduce structural constraints.

MAGP-1 is one of the few matrix proteins

that binds active TGF β without the involvement of glycosaminoglycans. Some ECM proteins, such as fibronectin, thrombospondin, fibulins, tenascins, and fibrillins, bind the large latent complex form of TGF β through interaction sites on the LTBP β s (9,40-43), although several bind the active isoform as well. In general, binding sites on matrix proteins for active TGF β are not well characterized, but the properties of the MAGP-1 growth factor binding domain may be instructive for identifying active sequences in these as well as other proteins. The microfibrillar protein emilin-1, for example, binds specifically to the proTGF β precursor and prevents its maturation by furin convertases (44). Growth factor binding activity was mapped to the protein's EMI domain, but the precise sequence was not identified nor is it clear whether the interaction is with the active or latent regions of the growth factor. Similarly, TGF β binding activity in the matricellular protein SPARC was localized in one study to the last 37 amino acids in the carboxy-terminal EC domain (45), but other work found that SPARC interacted with TGF β only when bound to its cognate type II receptor (46). Interestingly, both emilin-1 and SPARC have clusters of acidic amino acids in the putative TGF β binding regions that create a negatively charged sequence similar to the growth factor binding domain in MAGP-1.

Our mapping studies create a clearer picture of the functionality of the MAGP-1 amino terminus. The first four amino acids in the TGF β binding peptide p17-35 overlap with the last four amino acids of a peptide used to define the binding site for tropoelastin and collagen VI (amino acids 12-21 in our numbering scheme) (13). It is not known, however, if TE or collagen VI can affect the binding of TGF β . Although this amino-terminal region seems to be available to interact with numerous proteins noncovalently, there is a specificity to the binding since MAGP-1 does not bind TGF β 3, collagens I, II, or V, FGF9, FGF21 or the cytokines TNF α , IL-4, IL-13, and RANKL (13,17).

Our finding that MAGP-1 binds active TGF β but not the small latent precursor form of the growth factor suggests that MAGP-containing microfibrils have the potential to store active TGF β in addition to the large latent form that covalently binds to fibrillin. Association of

TGF β with MAGP-1 does not alter the growth factor's signaling potential, nor does an association between MAGP-1 and fibrillin alter MAGP-1's ability to bind TGF β . Thus, activated TGF β bound to MAGP-1 on microfibrils is capable of signaling when interacting with its receptor on cells and does not require an additional activation step to do so.

It is noteworthy that the absence of MAGP-1 or MAGP-2 (or both) is sufficient to raise the amount of total TGF β stored in the ECM of cultured cells. This finding is consistent with studies by Massam-Wu et al. (23), who showed the MAGP-1 could directly compete with LTBP-1 for binding to fibrillin. In the absence of MAGP, one would, therefore, expect more total TGF β to be associated with the ECM, which is what we found using MAGP knockout cells. Importantly, the presence of latent but not active TGF β in the ECM of MAGP-1:MAGP-2 double knockout cells suggests that in the absence of the MAGPs, active TGF β is not retained in the matrix.

The mechanistic and functional mapping studies described in this report, together with our previous characterization of MAGP knockout mouse phenotypes indicating increased TGF β activity, provide strong evidence for regulation of the TGF β pathway as one of MAGP's major functional roles in tissues.

EXPERIMENTAL PROCEDURES

Materials:

Carrier-free active TGF β -1 (7666-MB-CF), BMP-2 (355-BM-010/CF) and latent TGF β -1 (299-LT) were purchased from R&D systems, Minneapolis, MN. Antibodies to MAGP-1 and fibrillin-2 have been described (36,47,48). Simply Blue Coomassie G-250 was obtained from Thermo Fisher scientific. Antibodies to Smad2/3 (5678S) and phospho-Smad2 (18338S) were from Cell Signaling, Danvers, MA.

Cell culture and TGF β -1 activity assay:

The TGF β reporter cell line MFB-F11 was a generous gift from Tony Wyss-Coray, Stanford University. The cells were routinely cultured in DMEM supplemented with non-essential amino acid, 10% fetal calf serum, and 100 μ g/ml

hygromycin B (Invitrogen, Carlsbad CA). On the afternoon before an assay, the cells were split into a 96 well assay plate (4×10^4 cells per well) and cultured overnight in the absence of hygromycin. For the assay, cells were rinsed in DMEM then incubated for 1 hour in DMEM-BSA (DMEM + 1.0 mg/ml heat-denatured BSA). To determine if MAGP-1 or the p17-35 peptide inhibits TGF β signaling, TGF β (80pM) was mixed with varying concentrations of MAGP-1 protein or p17-35 peptide in DMEM-BSA for 30 minutes at room temperature then incubated with the reporter cells for 24 h. Soluble alkaline phosphatase released into the media in response to TGF β was measured using the Phospha-Light™ SEAP Reporter Gene Assay System (Life Technologies).

MEF and MFB-F11 co-culture

Levels of active and total TGF β in the ECM of cultured MEFs were assessed using established methods (20,49). Embryonic fibroblasts from wild type and MAGP-1 knockout mice were generated from explants as previously described (18). Early passage cells (passage 4 or less) were maintained in DMEM with 10% fetal calf serum supplemented with non-essential amino acids and routinely passaged 1:3 at confluence. For growth factor measurements, cells were plated at confluence in replicate 12 well tissue culture dishes and maintained for 14 days prior to TGF β assays. The cells were rinsed with PBS and incubated for 1 hr in DMEM containing 1 mg/ml of heat denatured BSA. For measurement of active TGF β levels, approximately 1×10^5 MFB-F11 reporter cells in DMEM-heat denatured BSA were added to the cultured MEF cells and incubated overnight. Supernatant from this co-culture was assayed for alkaline phosphatase using the Phospha-Light™ SEAP Reporter Gene Assay System (Life Technologies).

To determine total protein and total TGF β , MEF cells were rinsed with PBS and the cell layer incubated in 250 μ l 0.2M HCl per well for 1 hour on ice. An aliquot was removed for total protein determination and the remaining solution neutralized by the addition of an equimolar amount of NaOH. The cell-layer extract was diluted 1:100 in DMEM containing 1mg/ml heat denatured BSA and assayed for TGF β using MFB-F11 cells as described above. The samples taken for protein determination were dried,

hydrolyzed in 6N HCl for 48 hours, and amine content measured with ninhydrin (50).

Smad2 phosphorylation:

RFL-6 cells were plated at a confluent density and incubated overnight in Ham's F12 medium containing 0.5% horse serum followed by a 1-hour incubation with Ham's F12 containing 0.1mg/ml heat denatured BSA to decrease background TGF β activity. TGF β -1 (50pM) was mixed with 0, 0.4, 20, or 1000nM MAGP-1 in Ham's F12 containing 0.1mg/ml heat denatured BSA for 1 hour at 37°C then added to the RFL-6 cells for 15 minutes. Cells were lysed in buffer containing 20mM Tris, pH 7.5, 150mM NaCl, 1mM EDTA, 1mM EGTA, 1% Triton X-100, 2.5mM sodium pyrophosphate, 1mM β -glycerophosphate, 1mM Na₃VO₄, 1mM NaF 1 \times protease inhibitor (Roche Applied Science). Lysates were cleared by centrifugation, and protein concentration determined. Eight μ g of lysate was run per lane on 10% SDS-PAGE gels then transferred to nitrocellulose membranes. Membranes were blocked in 1% casein then incubated overnight with the indicated primary antibodies. Antibodies were detected with secondary antibodies conjugated to horse radish peroxidase and visualized using chemiluminescent substrate (Millipore WBKLS0100). The standards used were Precision Plus Dual Color protein standards (Biorad 161-0374)

MAGP-1 recombinant expression constructs:

Mouse MAGP-1 cDNA was amplified from a full-length clone (IMAGE:5249342) using a forward primer with a SphI restriction site added to the 5' end (full-length forward primer with SphI) and a reverse primer with SacI restriction site added to 3' end (full-length reverse primer with SacI). The resultant amplification product along with pQE31 was digested with SphI and SacI, gel purified, and appropriate bands ligated. The ligation mix was used to transform the M15 strain of *E-coli*, and a bacterial colony containing a plasmid with the appropriate sequence was used for expression.

A fragment of MAGP-1 representing domains 3-4 was amplified from the full-length pQE31 construct using a forward primer (truncation forward) from pQE31 sequence and a

reverse primer from the MAGP-1 sequence containing a SacI restriction site (Exon 4 reverse with SacI). The amplification product, along with pQE31 was digested with EcoRI and SacI, gel purified, and appropriate bands extracted and ligated. Fragments for domain 4-9 and 5-9 truncations were amplified from the full-length construct using a reverse primer from pQE31 (truncation reverse) sequence and a forward primer from MAGP-1 sequence containing a BamHI restriction site (exon 4 forward with BamHI or exon 5 forward with BamHI). The amplification products were digested along with pQE31 with BamHI and SacI, gel purified, and the appropriate bands ligated. The ligation mix from each construct was used to transform M15 *E. coli*. Colonies were picked from the transformations and sequence verified. The primer sequences used to construct 6-His full-length and truncated MAGP-1 are:

Full-length forward primer with SphI:

TAGCATGCTCAGGGCCAATATGACCTGGA,

Full-length reverse primer with SacI:

TAGAGCTCCTAGCAGCCCCACAGCTCC TG

Truncation forward:

CACACAGAATTCATTAAGAGGAG

Exon 4 reverse with SacI:

CAGAGCTCTTGGTAGTCATAGTAGTCTG

Exon 4 forward with BamHI

CAGGATCCTGACAACGCAGACTACTATG

Exon 5 forward with BamHI:

CAGGATCCAGAAGTGAGTCCTCGG

Truncation reverse:

TTAAGCTTGGCTGCAGGT

Peptides, protein expression and purification:

6-His-tagged fusion proteins were expressed and purified using the Qiagen expression system (Qiagen Inc. Valencia, CA). Bacteria expressing full-length or truncated protein were expanded, and while in log-phase, induced with IPTG at 1mM final concentration for 4 hours at 30°C. The bacteria were collected by centrifugation, extracted overnight at 4°C with gentle agitation in TRIS-phosphate buffered urea (8M pH8.0) containing protease inhibitors. After clarifying the extract by centrifugation (12,000xg for 20 minutes), recombinant 6-His containing

proteins were isolated with nickel resin chromatography. Proteins were refolded on the column (51), and eluted with a 0-300mM imidazole gradient in 50mM TRIS pH7.4. Fractions were analyzed by SDS-PAGE, and fractions containing protein were dialyzed against water and lyophilized. The fusion-proteins were further purified using HPLC over a PRP-3 reverse-phase column using a 0-30% acetonitrile gradient in 0.05% triethylamine. The protein content of purified proteins was determined by absorbance at 280nm using an extinction coefficient based on the protein sequence (DNASTar, Madison WI). The purity of the expressed proteins was assessed using SDS-PAGE with reducing (10mM DTT) sample buffer on 8-25% gradient Phastgels (GE Healthcare Life Sciences Pittsburgh, PA) and stained with Simply Blue (Invitrogen). Peptides were synthesized by Genscript (Piscataway, NJ) and further purified using HPLC over a PRP-3 reverse-phase column using a 0-30% acetonitrile gradient in 0.05% triethylamine. Fractions were dried and analyzed by amino acid analysis.

RNA isolation and quantitative PCR:

RNA was isolated using a RNeasy kit (Qiagen74104) after cell homogenization using QIAshredder (Qiagen 79656). cDNA was generated using the high capacity RNA-to-cDNA kit (Applied Biosystems 4387406). Quantitative PCR was performed on a ViiA7 (Applied Biosystems) using reagents and taqman probes supplied by Applied Biosystems for GAPDH (Mm99999915G1) and TGFβ (Mm01178820_m1). Quadruplicate measurements from 100ng RNA were performed for each sample.

Purification of Fibrillin-2

Fifty ml of serum-free conditioned medium from SF-9 cells expressing full-length fibrillin-2 (manuscript in preparation) was applied at a flow rate of 4ml/min onto a 1.0 x 9.5 cm Source 15Q strong anion exchange column (GE Healthcare) at room temperature using a Pharmacia FPLC system. The column was washed with 50ml buffer A (buffer A: 25mM HEPES, 0.1mM CaCl₂ pH7.4) followed by a 10ml gradient from 0-25% buffer B (buffer B: 25mM HEPES, 0.1mM CaCl₂, 1.0M NaCl pH7.4). Fibrillin-2,

which remained bound to the resin, was eluted with a 50ml 25-50% linear buffer B gradient before the column was recycled with 15ml 100% buffer B and 100ml buffer A. The elution stream was monitored for protein at 228 nm and NaCl content using conductivity. Each fraction was assessed for fibrillin-2 using an antifibrillin-2 antibody via dot-blot and densitometry with ImageJ. The three peak fractions containing fibrillin-2 were pooled and further purified on a 1.6 cm x 1.6 m Sephacryl S-500 column (fractionation range 40 - 20,000 KDa) equilibrated in 25mM HEPES, 125mM NaCl 0.1mM CaCl₂ pH7.4. The column flow rate was 1ml/min at 4°C, and 6ml fractions were collected. The elution stream was monitored for protein at 280nm and fibrillin-2 content for each fraction was determined by dot-blot. The final product was analyzed by SDS-PAGE on a 4% polyacrylamide gel with Laemmli buffer in the presence and absence of a reducing agent. Duplicate gels were either stained with Simply Blue Coomassie G-250 or transferred to nitrocellulose and stained for fibrillin-2 by western blot. The purity of the fibrillin-2 is shown in supplemental figure 3. The standards used were Precision plus dual color protein standards (Bio-Rad inc.). The western blot detection used a secondary donkey anti-rabbit antibody-HRP conjugate (Amersham Inc.) that was visualized on film using a chemiluminescent substrate (Millipore Corporation).

Surface plasmon resonance:

Initial mapping of the TGFβ-1 binding site in MAGP-1 was accomplished using a Biacore X to measure the change in surface plasmon resonance due to the interaction of TGFβ-1 in solution with expressed full-length MAGP-1 or truncated MAGP-1 fragments coupled to a CM5 chip. For coupling, the protein was dissolved at 20 µg/ml in 5mM acetate buffer, pH4.5, and injected for 10 minutes onto a CM5 sensor chip previously activated for 10 minutes with 0.05M NHS-0.2M EDC. Reactive sites on the chip were quenched with 100ul of 100mM ethanolamine pH=8.0 then the chip was equilibrated in HBST running buffer (10mM HEPES 150mM NaCl pH=7.4 containing .01% triton-100). Varying concentrations of TGFβ-1 diluted in running buffer were then injected. The volume of TGFβ-

1 injected was 60ul, and the flow rate was 20ul/minute. The precise localization of the growth factor binding site in MAGP-1 was determined using inhibition of TGFβ-1 binding to full-length MAGP-1 by synthetic peptides. These experiments and the latent TGFβ binding studies were performed on a Reichert SR7000DC SPR system. Full-length MAGP-1 was coupled to a carboxymethyl dextran hydrogel surface sensor chip using the same coupling conditions used for the Biacore CM-5 chip. TGFβ-1 or BMP-2 (50nM final concentration) was mixed with varying concentrations of MAGP-1 synthetic peptide at room temperature for at least 15 minutes prior to injection. The flow rate for the localization studies was 50 µl/minute, and the injection volume was 100ul.

Latent TGFβ-1 (5uM stock solution) was diluted to 15nM in HBST and injected over the MAGP-1 chip. To activate the latent TGFβ-1, HCl was added to the latent TGFβ-1 stock solution to a final concentration of 100mM for 15 minutes at room temperature followed by neutralization with the addition of an equimolar concentration of NaOH. The activated TGFβ-1 was diluted to 15nM in HBST and injected over the full-length MAGP-1 chip.

In ternary complex studies, fibrillin-2 was diluted 1:5 in 5mM sodium acetate and coupled with repeat 250ul injections onto a CM-5 activated and blocked as described above. Approximately 4000uRIU were coupled to the chip. Direct binding of TGFβ-1 and BMP-2 to fibrillin-2 was initially assessed prior to loading MAGP-1 onto the fibrillin-2 chip. After direct binding experiments, the chip was recycled, and MAGP-1 was loaded onto the chip with duplicate MAGP-1 injections (100ul injection at 500nM) where approximately 130uRU bound. Binding of TGFβ-1 and BMP-2 to the complex of fibrillin-2 and MAGP-1 was then re-assessed. No recycling was performed between injections on the fibrillin-2 MAGP-1 complex. HBST was used as the sample dilution buffer as the mobile phase. Unless otherwise noted, chips were recycled with 50ul injections of 0.2M glycine pH=2.3.

MAGP peptide structure prediction

The MAGP-1 p17-35 region that was experimentally determined to bind to TGFβ was analyzed for potential secondary structure and

disorder. Secondary structure was predicted using Jpred4 (52), Psipred (53), and DISOPRED (54). Additionally, the sequence was analyzed using IUPred2A (55). Structural predictions were performed using PEP-FOLD and PEP-FOLD3 (56,57)

MAGP-TGF β interaction predictions

TGF β family structures were downloaded from the protein data bank 1TGK (58), 4KV5 (59), 1KLA, 1KLC, 1KLD (60). Structures were edited to delete any additional ligands or binding partners. When appropriate, structures were subjected to energy minimization in NAMD (61) to produce a relaxed structure. Based on

experimental SPR results from the lab, the MAGP-1 p17-35 sequence were chosen as docking candidates. The sequences were treated as flexible peptides and were docked to the TGF β structures using GalaxyDock (62) and CABS-dock (63). Predicted structures were evaluated by score and feasibility. Structures were manually compared to structures of known TGF β -containing complexes, specifically receptor bound TGF β 3KFD (64) and TGF β in the large latent complex 3RJR (65), 5VQP (66). Structures were visualized using VMD (67) and VMD was used to generate all images.

ACKNOWLEDGEMENTS

We thank Dr. Tony Wyss-Coray, Department of Neurology and Neurological Sciences, Stanford University, for providing the TGF β reporter cell line MFB-F11.

CONFLICT OF INTEREST

The authors declare that they have no conflicts of interest with the contents of this article. The content is solely the responsibility of the authors and does not necessarily represent the official views of the National Institutes of Health

REFERENCES

1. Hynes, R. (2009) The extracellular matrix: not just pretty fibrils. *Science* **326**, 1216-1219
2. Robertson, I., Jensen, S., and Handford, P. (2011) TB domain proteins: evolutionary insights into the multifaceted roles of fibrillins and LTBP. *Biochem J* **433**, 263-276
3. Davis, E. C., Roth, R. A., Heuser, J. E., and Mecham, R. P. (2002) Ultrastructural properties of ciliary zonule microfibrils. *J. Struct. Biol.* **139**, 65-75
4. Goldfischer, S., Coltoff-Schiller, B., and Goldfischer, M. (1985) Microfibrils, elastic anchoring components of the extracellular matrix, are associated with fibronectin in the zonule of Zinn and aorta. *Tissue Cell* **17**, 441-450
5. Wagenseil, J., and Mecham, R. (2009) Vascular extracellular matrix and arterial mechanics. *Physiol. Rev.* **89**, 957-989
6. McConnell, C., DeMont, M., and Wright, G. (1997) Microfibrils provide non-linear elastic behaviour in the abdominal artery of the lobster *Homarus americanus*. *J. Physiol.* **499** 513-526
7. Davison, I., Wright, G., and DeMont, M. (1995) The structure and physical properties of invertebrate and primitive vertebrate arteries. *J. Exp. Biol.* **198**, 2185-9216
8. Isogai, Z., Ono, R. N., Ushiro, S., Keene, D. R., Chen, Y., Mazzieri, R., Charbonneau, N. L., Reinhardt, D. P., Rifkin, D. B., and Sakai, L. Y. (2003) Latent transforming growth factor beta-binding protein 1 interacts with fibrillin and is a microfibril-associated protein. *J. Biol. Chem.* **278**, 2750-2757
9. Robertson, I., Horiguchi, M., Zilberberg, L., Dabovic, B., Hadjiolova, K., and Rifkin, D. (2015) Latent TGF- β -binding proteins. *Matrix Biol* **47**, 44-53
10. Travis, M., and Sheppard, D. (2014) TGF-beta activation and function in immunity. *Annu Rev Immunol* **32**, 51-82
11. Carta, L., Pereira, L., Arteaga-Soli, E., Lee-Arteaga, S. Y., Lenart, B., Starcher, B., Merkel, C. A., Sukoyan, M., Kerkis, A., Hazeki, N., Keene, D. R., Sakai, L. Y., and Ramirez, F. (2006) Fibrillins 1 and 2 perform partially overlapping functions during aortic development. *J. Biol. Chem.* **281**, 8016-8023
12. Brown-Augsburger, P., Broekelmann, T., Mecham, L., Mercer, R., Gibson, M. A., Cleary, E. G., Abrams, W. R., Rosenbloom, J., and Mecham, R. P. (1994) Microfibril-associated glycoprotein (MAGP) binds to the carboxy-terminal domain of tropoelastin and is a substrate for transglutaminase. *J. Biol. Chem.* **269**, 28443-28449
13. Finnis, M. L., and Gibson, M. A. (1997) Microfibril-associated glycoprotein-1 (MAGP-1) binds to the pepsin-resistant domain of the alpha3(VI) chain of type VI collagen. *J. Biol. Chem.* **272**, 22817-22823
14. Werneck, C. C., Trask, B. C., Broekelmann, T. J., Trask, T. M., Ritty, T. M., Segade, F., and Mecham, R. P. (2004) Identification of a major microfibril-associated glycoprotein-1-binding domain in fibrillin-2. *J. Biol. Chem.* **279**, 23045-23051
15. Craft, C., Pietka, T., Schappe, T., Coleman, T., Combs, M., Klein, S., Abumrad, N., and Mecham, R. (2014) The extracellular matrix protein MAGP1 supports thermogenesis and protects against obesity and diabetes through regulation of TGF-beta. *Diabetes* **63**, 1920-1932
16. Combs, M., Knutsen, R., Broekelmann, T., Toennies, H., Brett, T., Miller, C., Kober, D., Craft, C., Atkinson, J., Shipley, J., Trask, B., and Mecham, R. (2013) Microfibril-associated glycoprotein 2 (MAGP2) loss of function has pleiotropic effects in vivo. *J Biol Chem* **288**, 28869-28880
17. Craft, C. S., Broekelmann, T. J., Zou, W., Chappel, J. C., Teitelbaum, S. L., and Mecham, R. P. (2012) Oophorectomy-induced bone loss is attenuated in MAGP1-deficient mice. *J Cell Biochem* **113**, 93-99
18. Weinbaum, J., Broekelmann, T., Pierce, R., Werneck, C., Segade, F., Craft, C., Knutsen, R., and Mecham, R. (2008) Deficiency in Microfibril-associated Glycoprotein-1 Leads to Complex

- Phenotypes in Multiple Organ Systems. *J Biol Chem* **283**, 25533-25543
19. Trask, B. C., Broekelmann, T. J., and Mecham, R. P. (2001) Post-translational modifications of microfibril associated glycoprotein-1 (MAGP-1). *Biochem.* **40**, 4372-4380
 20. Tesseur, I., Zou, K., Berber, E., Zhang, H., and Wyss-Coray, T. (2006) Highly sensitive and specific bioassay for measuring bioactive TGF-beta. *BMC Cell Biol* **7**, 15
 21. Shi, M., Zhu, J., Wang, R., Chen, X., Mi, L., Walz, T., and Springer, T. (2011) Latent TGF-beta structure and activation. *Nature* **474**, 343-349
 22. Kanzaki, T., Olofsson, A., Moren, A., Wernstedt, C., Hellman, U., Miyazono, K., Claesson-Welsh, L., and Heldin, C. H. (1990) TGF-beta 1 binding protein: a component of the large latent complex of TGF-beta 1 with multiple repeat sequences. *Cell* **61**, 1051-1061
 23. Massam-Wu, T., Chiu, M., Choudhury, R., Chaudhry, S., Baldwin, A., McGovern, A., Baldock, C., Shuttleworth, C., and Kielty, C. (2010) Assembly of fibrillin microfibrils governs extracellular deposition of latent TGF beta. *J Cell Sci* **123**, 3006-3018
 24. Broekelmann, T. J., Limper, A. H., Colby, T. V., and McDonald, J. A. (1991) Transforming growth factor beta 1 is present at sites of extracellular matrix gene expression in human pulmonary fibrosis. *Proc Natl Acad Sci U S A* **88**, 6642-6646
 25. Hinz, B. (2015) The extracellular matrix and transforming growth factor-beta1: Tale of a strained relationship. *Matrix Biol* **47**, 54-65
 26. ten Dijke, P., and Arthur, H. (2007) Extracellular control of TGFbeta signalling in vascular development and disease. *Nat Rev Mol Cell Biol* **8**, 857-869
 27. Mecham, R. P., and Gibson, M. A. (2015) The microfibril-associated glycoproteins (MAGPs) and the microfibrillar niche. *Matrix Biol* **47**, 13-33
 28. Craft, C. S., Broekelmann, T. J., and Mecham, R. P. (2018) Microfibril-associated glycoproteins MAGP-1 and MAGP-2 in disease. *Matrix Biol* **71-72**, 100-111
 29. Villain, G., Lelievre, E., Broekelmann, T., Gayet, O., Havet, C., Werkmeister, E., Mecham, R., Dusetti, N., Soncin, F., and Mattot, V. (2018) MAGP-1 and fibronectin control EGFL7 functions by driving its deposition into distinct endothelial extracellular matrix locations. *FEBS J*
 30. Craft, C., Zou, W., Watkins, M., Grimston, S., Brodt, M., Broekelmann, T., Weinbaum, J., Teitelbaum, S., Pierce, R., Civitelli, R., Silva, M., and Mecham, R. (2010) Microfibril-associated glycoprotein-1, an extracellular matrix regulator of bone remodeling. *J. Biol. Chem.* **285**, 23858-23867
 31. Walji, T. A., Turecamo, S. E., Sanchez, A. C., Anthony, B. A., Abou-Ezzi, G., Scheller, E. L., Link, D. C., Mecham, R. P., and Craft, C. S. (2016) Marrow Adipose Tissue Expansion Coincides with Insulin Resistance in MAGP1-Deficient Mice. *Front Endocrinol (Lausanne)* **7**, 87
 32. Liu, Y. J., Xu, F. H., Shen, H., Liu, Y. Z., Deng, H. Y., Zhao, L. J., Huang, Q. Y., Dvornyk, V., Conway, T., Davies, K. M., Li, J. L., Recker, R. R., and Deng, H. W. (2004) A follow-up linkage study for quantitative trait loci contributing to obesity-related phenotypes. *J. Clin. Endocrinol. Metab.* **89**, 875-882
 33. Barbier, M., Gross, M., Aubart, M., Hanna, N., Kessler, K., Guo, D., Tosolini, L., Ho-Tin-Noe, B., Regalado, E., Varret, M., Abifadel, M., Milleron, O., Odent, S., Dupuis-Girod, S., Faivre, L., Edouard, T., Dulac, Y., Busa, T., Gouya, L., Milewicz, D., Jondeau, G., and Boileau, C. (2014) MFAP5 Loss-of-Function Mutations Underscore the Involvement of Matrix Alteration in the Pathogenesis of Familial Thoracic Aortic Aneurysms and Dissections. *Am J Hum Genet* **95**, 736-743
 34. Segade, F., Trask, B. C., Broekelmann, T., Pierce, R. A., and Mecham, R. P. (2002) Identification of a matrix binding domain in MAGP1 and 2 and intracellular localization of alternative splice forms. *J. Biol. Chem.* **277**, 11050-11057
 35. Weinbaum, J., Tranquillo, R., and Mecham, R. (2010) The matrix-binding domain of microfibril-associated glycoprotein-1 targets active connective tissue growth factor to a fibroblast-produced extracellular matrix. *Macromol Biosci* **10**, 1338-1344
 36. Trask, B. C., Trask, T. M., Broekelmann, T., and Mecham, R. P. (2000) The microfibrillar

- proteins MAGP-1 and fibrillin-1 form a ternary complex with the chondroitin sulfate proteoglycan decorin. *Molec. Biol. Cell* **11**, 1499-1507
37. Reinboth, B., Hanssen, E., Cleary, E. G., and Gibson, M. A. (2002) Molecular interactions of biglycan and decorin with elastic fiber components: biglycan forms a ternary complex with tropoelastin and microfibril-associated glycoprotein 1. *J. Biol. Chem.* **277**, 3950-3957
 38. Lee, J., Wee, S., Gunaratne, J., Chua, R. J., Smith, R. A., Ling, L., Fernig, D. G., Swaminathan, K., Nurcombe, V., and Cool, S. M. (2015) Structural determinants of heparin-transforming growth factor-beta1 interactions and their effects on signaling. *Glycobiology* **25**, 1491-1504
 39. Lyon, M., Rushton, G., and Gallagher, J. T. (1997) The interaction of the transforming growth factor-betas with heparin/heparan sulfate is isoform-specific. *J Biol Chem* **272**, 18000-18006
 40. Smaldone, S., Clayton, N. P., del Solar, M., Pascual, G., Cheng, S. H., Wentworth, B. M., Schaffler, M. B., and Ramirez, F. (2016) Fibrillin-1 Regulates Skeletal Stem Cell Differentiation by Modulating TGFbeta Activity Within the Marrow Niche. *J Bone Miner Res* **31**, 86-97
 41. Dallas, S., Sivakumar, P., Jones, C., Chen, Q., Peters, D., Mosher, D., Humphries, M., and Kielty, C. (2005) Fibronectin regulates latent transforming growth factor-beta (TGF beta) by controlling matrix assembly of latent TGF beta-binding protein-1. *J. Biol. Chem.* **280**, 18871-11880
 42. Murphy-Ullrich, J. E., and Suto, M. J. (2018) Thrombospondin-1 regulation of latent TGF-beta activation: A therapeutic target for fibrotic disease. *Matrix Biol* **68-69**, 28-43
 43. Alcaraz, L. B., Exposito, J. Y., Chuvin, N., Pommier, R. M., Cluzel, C., Martel, S., Sentis, S., Bartholin, L., Lethias, C., and Valcourt, U. (2014) Tenascin-X promotes epithelial-to-mesenchymal transition by activating latent TGF-beta. *J Cell Biol* **205**, 409-428
 44. Zacchigna, L., Vecchione, C., Notte, A., Cordenonsi, M., Dupont, S., Maretto, S., Cifelli, G., Ferrari, A., Maffei, A., Fabbro, C., Braghetta, P., Marino, G., Selvetella, G., Aretini, A., Colonnese, C., Bettarini, U., Russo, G., Soligo, S., Adorno, M., Bonaldo, P., Volpin, D., Piccolo, S., Lembo, G., and Bressan, G. M. (2006) Emilin1 links TGF-beta maturation to blood pressure homeostasis. *Cell* **124**, 929-942
 45. Tumbarello, D. A., Andrews, M. R., and Brenton, J. D. (2016) SPARC Regulates Transforming Growth Factor Beta Induced (TGFBI) Extracellular Matrix Deposition and Paclitaxel Response in Ovarian Cancer Cells. *PLoS One* **11**, e0162698
 46. Francki, A., McClure, T. D., Brekken, R. A., Motamed, K., Murri, C., Wang, T., and Sage, E. H. (2004) SPARC regulates TGF-beta1-dependent signaling in primary glomerular mesangial cells. *J Cell Biochem* **91**, 915-925
 47. Brown-Augsburger, P. B., Broekelmann, T., Rosenbloom, J., and Mecham, R. P. (1996) Functional domains on elastin and MAGP involved in elastic fiber assembly. *Biochem. J.* **318**, 149-155
 48. Trask, T., Ritty, T., Broekelmann, T., Tisdale, C., and Mecham, R. (1999) N-terminal domains of fibrillin 1 and fibrillin 2 direct the formation of homodimers: a possible first step in microfibril assembly. *Biochem J* **340** 693-701
 49. Mazzieri, R., Munger, J. S., and Rifkin, D. B. (2000) Measurement of active TGF-beta generated by cultured cells. *Methods Mol Biol* **142**, 13-27
 50. Stoilov, I., Starcher, B. C., Mecham, R. P., and Broekelmann, T. J. (2018) Measurement of elastin, collagen, and total protein levels in tissues. *Methods Cell Biol* **143**, 133-146
 51. Hutchinson, M. H., and Chase, H. A. (2006) Adsorptive refolding of histidine-tagged glutathione S-transferase using metal affinity chromatography. *J Chromatogr A* **1128**, 125-132
 52. Drozdetskiy, A., Cole, C., Procter, J., and Barton, G. J. (2015) JPred4: a protein secondary structure prediction server. *Nucleic Acids Research* **43**, W389-W394
 53. Buchan, D. W. A., and Jones, D. T. (2019) The PSIPRED Protein Analysis Workbench: 20 years on. *Nucleic Acids Research* **47**, W402-W407
 54. Jones, D. T., and Cozzetto, D. (2014) DISOPRED3: precise disordered region predictions with annotated protein-binding activity. *Bioinformatics* **31**, 857-863
 55. Mészáros, B., Erdős, G., and Dosztányi, Z. (2018) IUPred2A: context-dependent prediction of

- protein disorder as a function of redox state and protein binding. *Nucleic Acids Research* **46**, W329-W337
56. Shen, Y., Maupetit, J., Derreumaux, P., and Tufféry, P. (2014) Improved PEP-FOLD Approach for Peptide and Miniprotein Structure Prediction. *Journal of Chemical Theory and Computation* **10**, 4745-4758
57. Thévenet, P., Shen, Y., Maupetit, J., Guyon, F., Derreumaux, P., and Tufféry, P. (2012) PEP-FOLD: an updated de novo structure prediction server for both linear and disulfide bonded cyclic peptides. *Nucleic Acids Research* **40**, W288-W293
58. Mittl, P. R., Priestle, J. P., Cox, D. A., McMaster, G., Cerletti, N., and Grütter, M. G. (1996) The crystal structure of TGF-beta 3 and comparison to TGF-beta 2: implications for receptor binding. *Protein science : a publication of the Protein Society* **5**, 1261-1271
59. Moulin, A., Mathieu, M., Lawrence, C., Bigelow, R., Levine, M., Hamel, C., Marquette, J.-P., Le Parc, J., Loux, C., Ferrari, P., Capdevila, C., Dumas, J., Dumas, B., Rak, A., Bird, J., Qiu, H., Pan, C. Q., Edmunds, T., and Wei, R. R. (2014) Structures of a pan-specific antagonist antibody complexed to different isoforms of TGFβ reveal structural plasticity of antibody–antigen interactions. *Protein Science* **23**, 1698-1707
60. Hinck, A. P., Archer, S. J., Qian, S. W., Roberts, A. B., Sporn, M. B., Weatherbee, J. A., Tsang, M. L. S., Lucas, R., Zhang, B.-L., Wenker, J., and Torchia, D. A. (1996) Transforming Growth Factor β1: Three-Dimensional Structure in Solution and Comparison with the X-ray Structure of Transforming Growth Factor β2. *Biochemistry* **35**, 8517-8534
61. Phillips, J. C., Braun, R., Wang, W., Gumbart, J., Tajkhorshid, E., Villa, E., Chipot, C., Skeel, R. D., Kalé, L., and Schulten, K. (2005) Scalable molecular dynamics with NAMD. *Journal of Computational Chemistry* **26**, 1781-1802
62. Lee, H., Heo, L., Lee, M. S., and Seok, C. (2015) GalaxyPepDock: a protein–peptide docking tool based on interaction similarity and energy optimization. *Nucleic Acids Research* **43**, W431-W435
63. Kurcinski, M., Pawel Ciemny, M., Oleniecki, T., Kuriata, A., Badaczewska-Dawid, A. E., Kolinski, A., and Kmiecik, S. (2019) CABS-dock standalone: a toolbox for flexible protein–peptide docking. *Bioinformatics* **35**, 4170-4172
64. Radaev, S., Zou, Z., Huang, T., Lafer, E. M., Hinck, A. P., and Sun, P. D. (2010) Ternary Complex of Transforming Growth Factor-β1 Reveals Isoform-specific Ligand Recognition and Receptor Recruitment in the Superfamily. *Journal of Biological Chemistry*, 14806-14814
65. Shi, M., Zhu, J., Wang, R., Chen, X., Mi, L., Walz, T., and Springer, T. A. (2011) Latent TGF-β structure and activation. *Nature* **474**, 343-349
66. Zhao, B., Xu, S., Dong, X., Lu, C., and Springer, T. A. (2017) Prodomain–growth factor swapping in the structure of pro-TGF-β1. *Journal of Biological Chemistry*, 1579-1589
67. Humphrey, W., Dalke, A., and Schulten, K. (1996) VMD: Visual molecular dynamics. *Journal of Molecular Graphics* **14**, 33-38

FOOTNOTES

Funding was provided by the National Institutes of Health grants HL-53325 and HL-105314, and the Ines Mandl Research Foundation, New York, New York. NKB was funded by National Institutes of Health training grants T32 HL125241 and T32 HL07317.

The abbreviations used are: DTT, dithiothreitol; IPTG, isopropyl β -D-1-thiogalactopyranoside; NHS, *N*-hydroxysuccinimide; EDC, *N*-(3-Dimethylaminopropyl)-*N'*-ethylcarbodiimide; SLC, small latent complex; LLC, large latent complex; HBST, HEPES buffered saline containing TritonX-100; SPR: surface plasmon resonance; RU: SPR response units; BSA, bovine serum albumin; MEF mouse embryonic fibroblasts

FIGURES

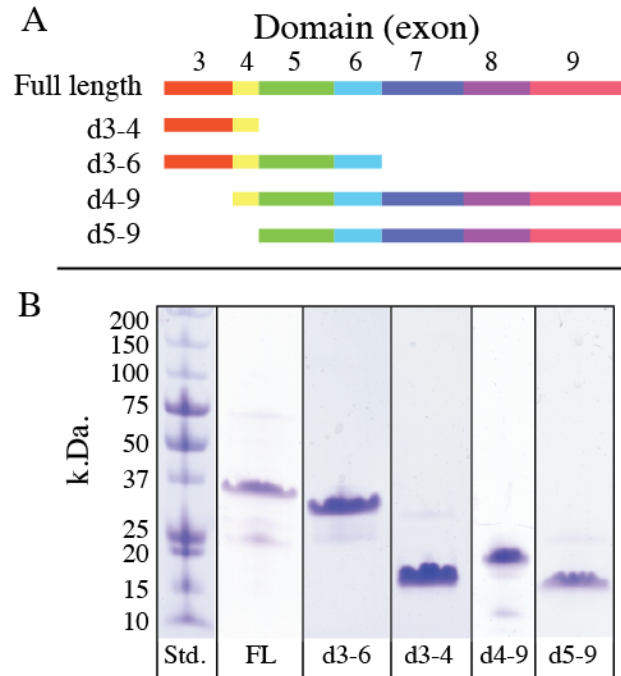


Figure 1. Domain structure of MAGP-1 and purity of expressed peptides. **A)** Full-length, secreted, MAGP-1 protein is encoded by seven exons (exons 3-9). In this report, each exon defines a protein domain, and truncations used for functional analysis were constructed based on exon boundaries. The schematic shows the domains included in the recombinant fragments (d followed by exon numbers). **B)** SDS-PAGE analysis of recombinant full-length MAGP-1 (FL) and purified truncated peptides shown in panel A. Proteins were separated on 8-25% Phastgels under reducing conditions and detected with Coomassie Brilliant Blue. The observed and expected molecular weights of each fragment are described in the Results section.

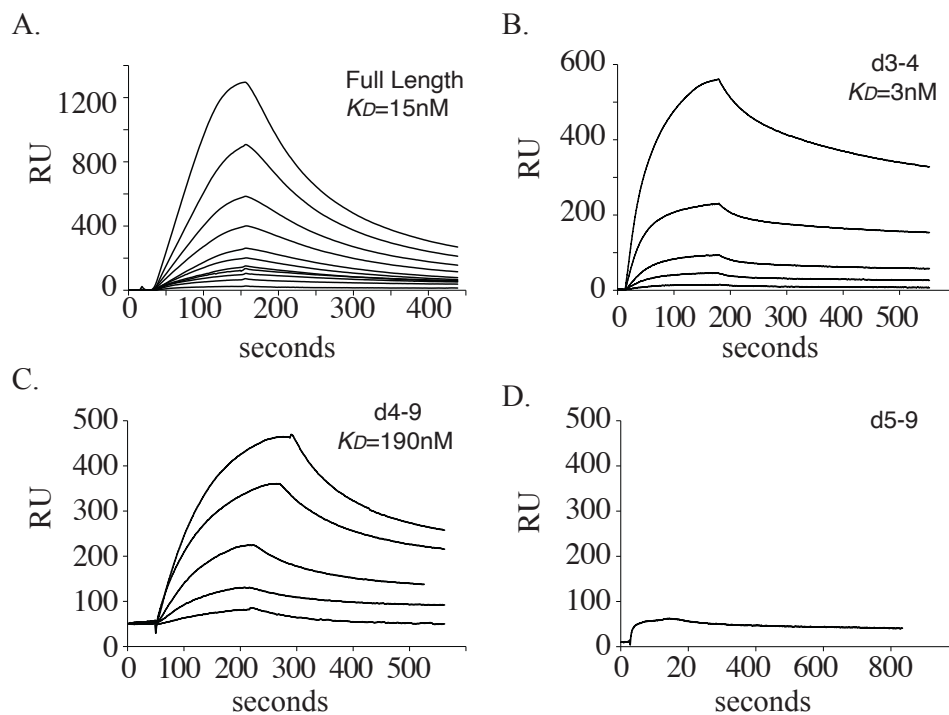


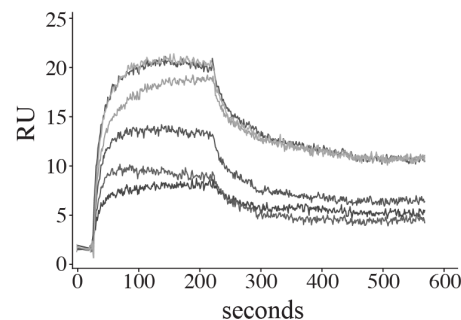
Figure 2. Binding of TGFβ-1 to purified full-length MAGP-1 or MAGP-1 fragments.

A) Graph of isotherms from the binding of TGFβ-1 to a CM5 chip coated with full-length MAGP-1 (2200 resonance units coupled). TGFβ-1 concentrations were, from the top, 100, 66.7, 44.4, 29.6, 19.8, 13.2, 8.8, 5.9, 3.9, 2.6, and 1.7 nM. **B-D)** show the interaction of TGFβ-1 (400, 200, 80, 67, 27 nM) with 440 resonance units of MAGP-1 domain protein 3-4 (**B**), with 4300 resonance units of MAGP-1 domain 4-9 (TGFβ-1 concentrations of 120, 60, 48, 24, 12 nM) (**C**), and 400nM TGFβ-1 with 2140 resonance units of MAGP-1 domain 5-9 (**D**).

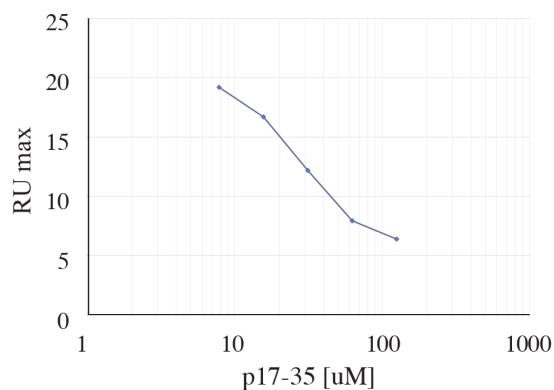
A.

activity	peptide	sequence
		-----domain 3----- domain 4-
+	p1-35	QGQYDLPLPFPDQVQYNHYGDQI-DNADYYDYQE
(-)	p1-18	QGQYDLPLPFPDQVQY-NH ₂
+	p12-37	FPDQVQYNHYGDQI-DNADYYDYQEVN-NH ₂
+	p17-35	QYNHYGDQI-DNADYYDYQE-NH ₂
(-)	p22-36	GDQI-DNADYYDYQEV
(-)	p26-35	DNADYYDYQE
(-)	p17-35pro	QYPHYPDQI-DNADYYDYQE-NH ₂

B.



C.



D.

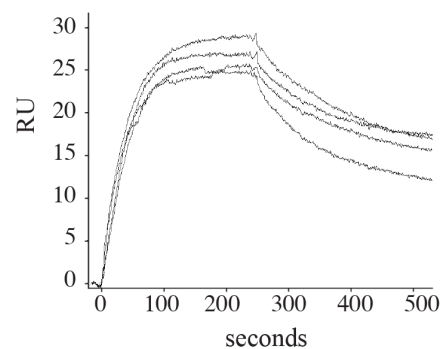


Figure 3. Fine mapping of TGF β -1 binding activity in domains 3-4. **A)** summarizes the inhibitory activity, the sequence and the location of the peptides tested for inhibition of TGF β -1 (50nM) binding to 120 units of full-length MAGP-1 coupled to a carboxymethyl dextran hydrogel surface sensor chip (MAGP-1 chip). **B)** is a graph of isotherms showing p17-35 dose-dependent inhibition of TGF β -1 binding to the MAGP-1-coated chip. **C)** relates the maximal binding of TGF β -1 (at 100 seconds) to the MAGP-1 chip in the presence of increasing concentrations of peptide p17-35 (taken from panel B). Isotherms in **D)** show that the control peptide p17-35pro (100, 50, 25 and 0 μ M) has no inhibitory effect on TGF β -1 binding to MAGP-1.

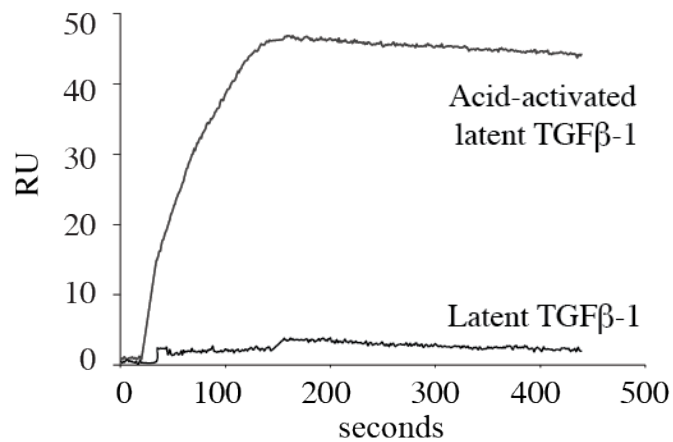


Figure 4. MAGP-1 does not bind latent TGFβ-1. Latent TGFβ-1 (15nM) was injected onto a MAGP-1 chip, and no interaction was detected. A second sample of latent TGFβ-1 was treated with 100mM HCl for 10 minutes at room temperature, neutralized with 100mM NaOH, and then diluted to a final concentration of 15nM. The binding isotherm shows that the acid-activated TGFβ-1 bound with high affinity to the MAGP-1 chip. The injection volume was 225 μl, and the flow rate was 50 μl/minute for both injections.

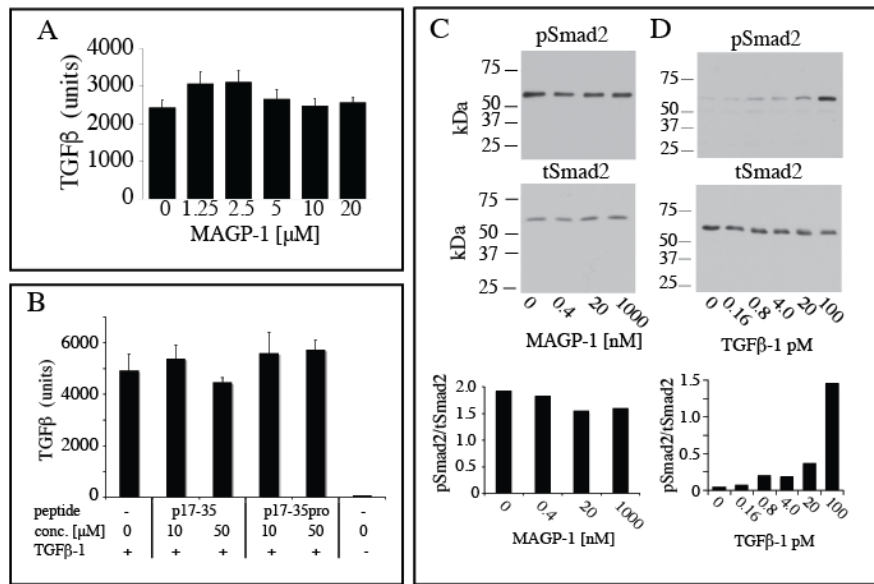


Figure 5. MAGP-1 and p17-35 do not block TGFβ-1 signaling. **A)** Active TGFβ-1 (80pM) was mixed with the indicated concentrations of MAGP-1, incubated for 15 minutes, and then added to MFB-F11 cells for 24 hours. The culture medium was then assayed for alkaline phosphatase activity, which provides a measure of TGFβ activity. Shown are mean \pm standard deviation, n=8. **B)** Active TGFβ-1 (80pM) was mixed with 10 μ M or 100 μ M p17-35, p17-35pro, or no peptide for 15 minutes and added to MFB-F11 cells for 24 hours. A control with no added TGFβ-1 was included. The medium was collected and assayed for alkaline phosphatase activity. Shown are mean \pm standard deviation, n=4. One-way analysis of variance showed no differences between samples in panels A or B. **C)** Increasing concentrations of soluble MAGP-1 were pre-incubated for 1 hour with 50pM TGFβ-1 and the complex incubated with RFL-6 cell (a fibroblast line that does not make MAGP-1) for 15 minutes. Cell extracts were then analyzed by western blot for phosphoSmad2 (pSmad-2) (top) and for total Smad2 (tSmad2) (bottom). The ratio of pSmad2 to tSmad2 is shown in the bottom graph. **D)** Smad2 phosphorylation in RFL-6 cells is TGFβ-1 dose dependent with minimal baseline phosphorylation. RFL-6 cells were treated with the indicated dose of TGFβ-1 and levels of phosphorylated Smad-2 (top panel) or total Smad-2 (bottom panel) were determined from cell extracts by western blot analysis. The ratio of pSmad2 to tSmad2 is shown in the bottom graph.

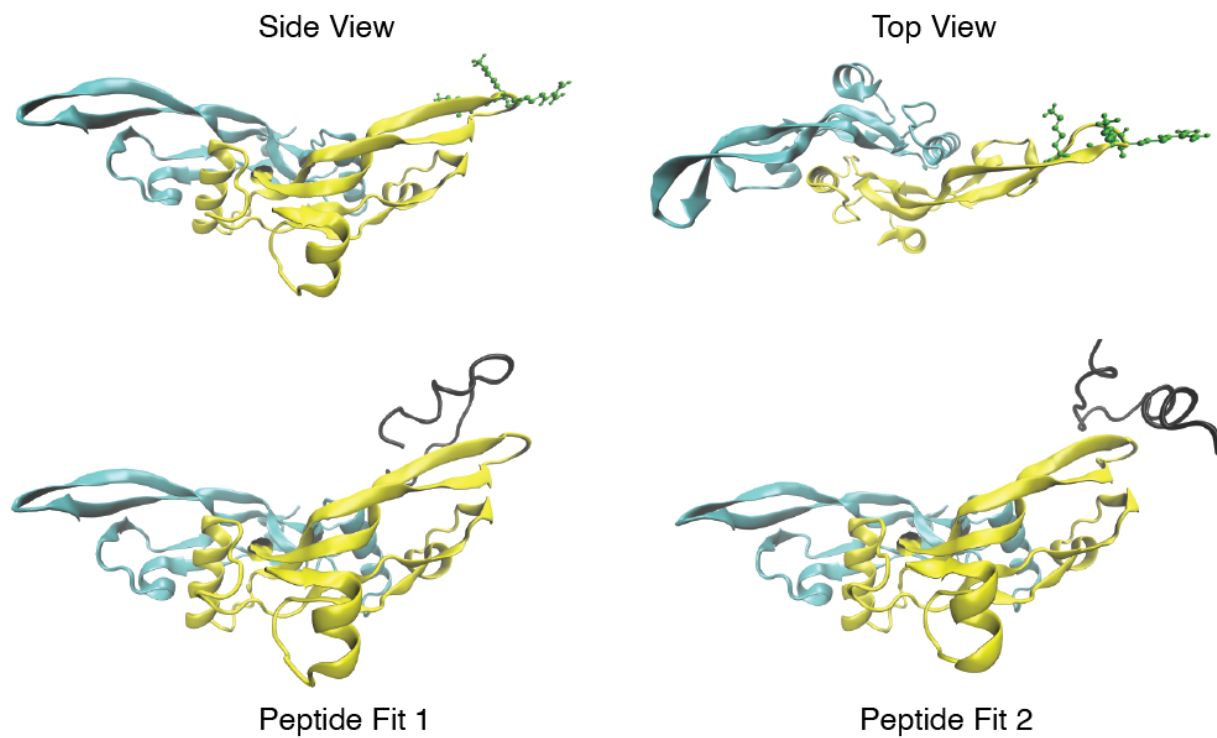


Figure 6: The structure of TGF β -1 with and without the MAGP-1 p17-35 peptide. Top: Side and top views of the TGF β -1 dimer with solvent exposed residues R94, K95, and K97 shown in green. **Bottom:** Representative binding of the MAGP-1 p17-35 peptide (shown in black) to TGF β -1. The MAGP-1 peptide remains largely disordered while consistently interacting with the positive residues in the TGF β -1 finger region.

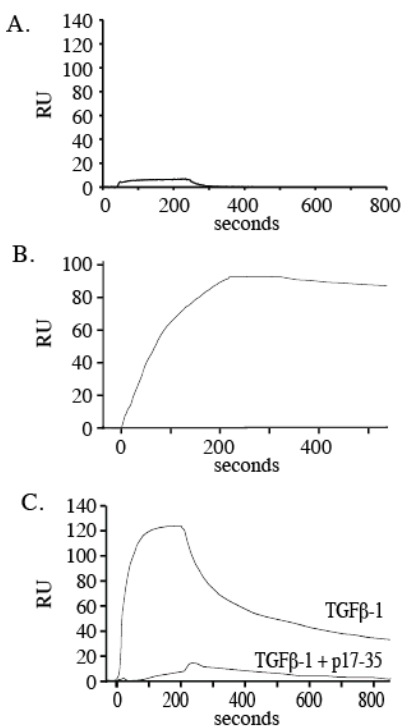


Figure 7. TGFβ-1 binds to fibrillin-2 only in the presence of MAGP-1. **A)** Purified full-length fibrillin-2 was covalently coupled (3,000 resonance-units) to a carboxymethyl dextran hydrogel surface sensor chip (fibrillin-2 chip), and TGFβ-1 was injected at a concentration of 50nM at 25ul per minute for 3.5 minutes. Data show no measurable interaction between the two proteins. **B)** MAGP-1 (6.2nM for 3.5 minutes at 25ul/min) bound to fibrillin-2 with an apparent affinity of 100pM. **C)** TGFβ-1 (50nM for 3.5 minutes at 25ul/min) bound to the MAGP-1-fibrillin-2 complex whereas TGFβ-1 pre-incubated with 50μM p17-35 peptide failed to bind to the complex.

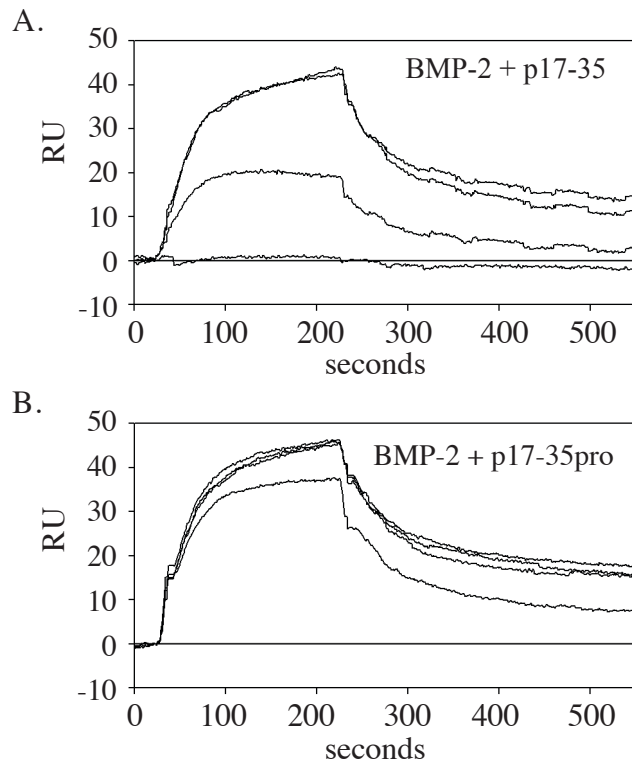


Figure 8. BMP-2 binding localizes to the same domain on MAGP-1 as TGF β -1. **A)** shows isotherms documenting binding of 50nM BMP-2 to a MAGP-1-coated chip. **B)** Binding was inhibited by preincubation of BMP-2 with peptide p17-35 from the top 0, 5, 25, and 50uM) but not the control peptide p17-35pro (0, 5, 25 and 50uM)

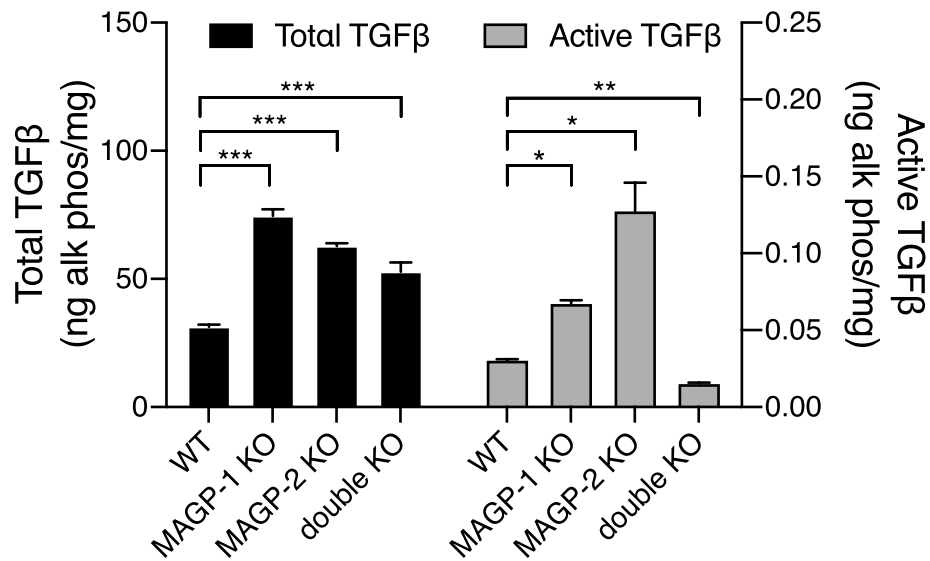


Figure 9. MAGP 1 and MAGP-2 modulate TGFβ levels in fibroblast ECM. Comparison of total TGFβ levels (black bars) in 14 day post confluent WT and MAGP knockout cell layers showing significant increases in total TGFβ in MAGP-1 knockout (** $p > 0.01$, $n=3$), MAGP-2 knockout (* $p > 0.05$, $n=3$), and MAGP-1;MAGP-2 double knockout (** $p > 0.01$) fibroblasts. Similarly, active TGFβ levels (grey bars) are significantly increased in MAGP-1 knockout (* $p > .05$, $n=2$) and MAGP-2 knockout (* $p > .05$, $n=3$) cells, but are decreased (** $P > .01$ $n=3$) in the double knockouts.

**Identification of the growth factor binding sequence in the extracellular matrix
protein MAGP-1**

Thomas J Broekelmann, Nicholas K Bodmer and Robert P Mecham

J. Biol. Chem. published online January 27, 2020

Access the most updated version of this article at doi: [10.1074/jbc.RA119.010540](https://doi.org/10.1074/jbc.RA119.010540)

Alerts:

- [When this article is cited](#)
- [When a correction for this article is posted](#)

[Click here](#) to choose from all of JBC's e-mail alerts